585 **Supplemental Information**

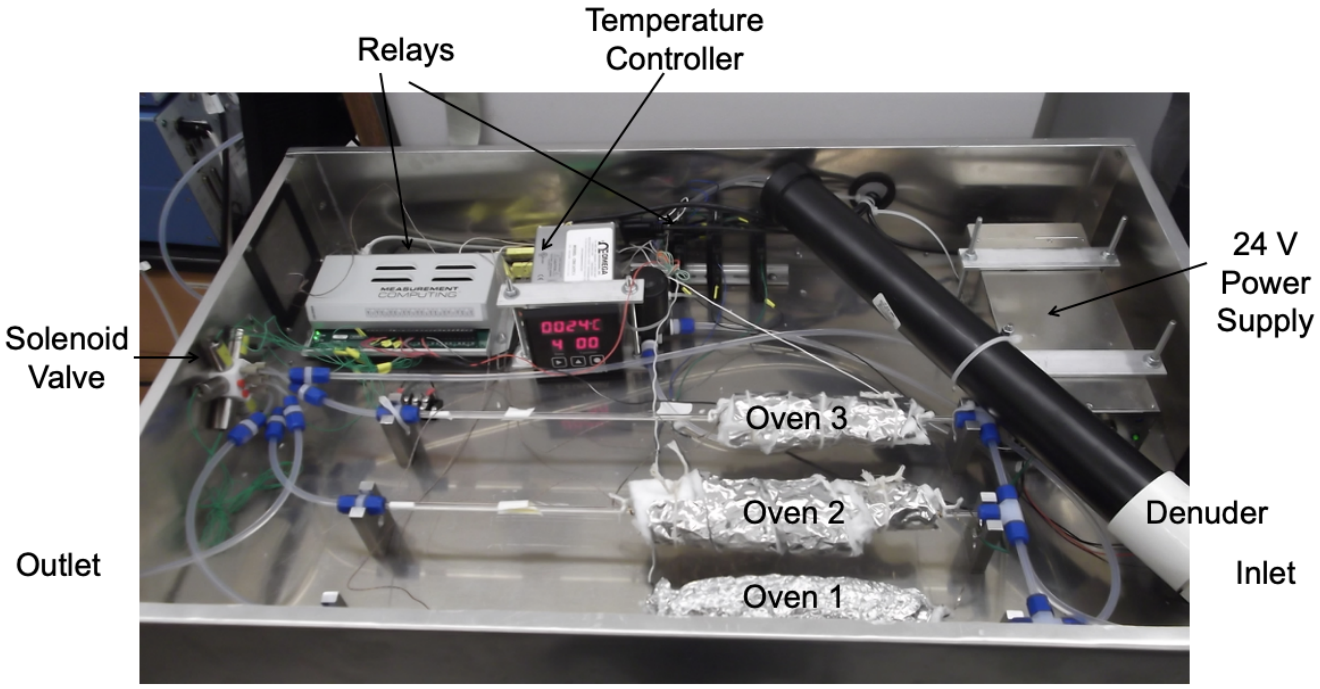

Figure S1. Oven inlet box.

590

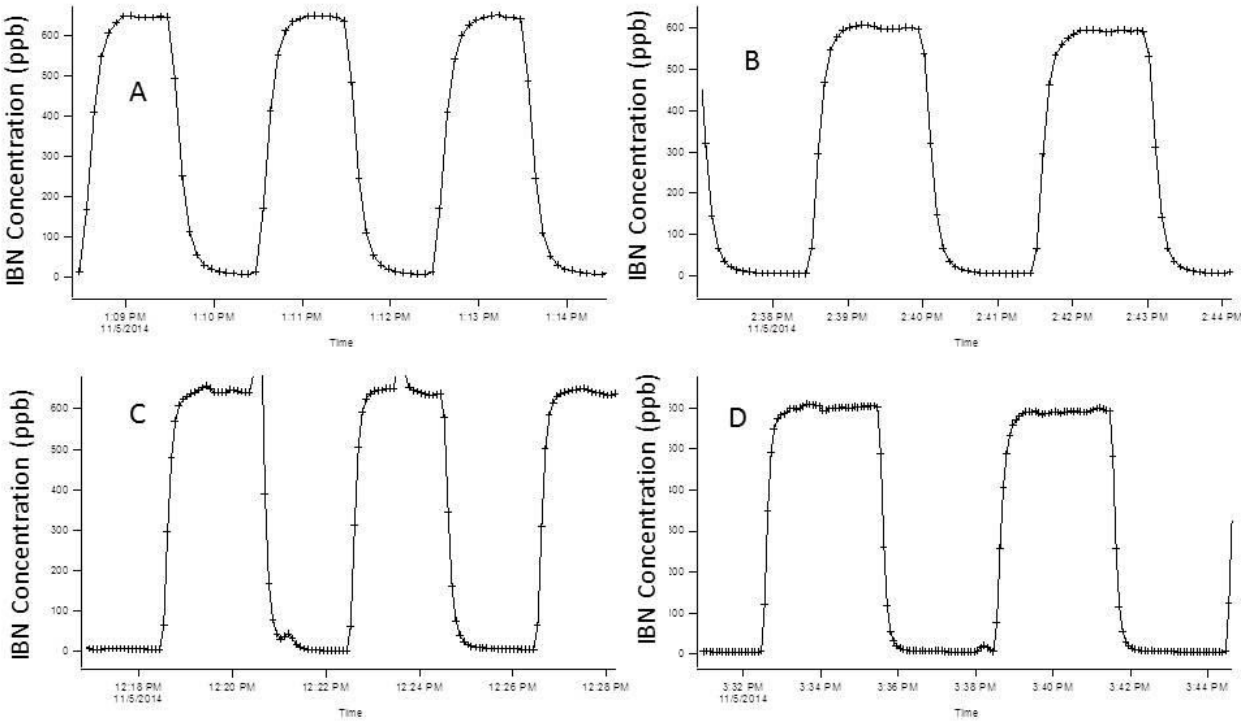

Figure S2. Channel switching frequency testing. Panel A shows 30 second sampling time, B 45 seconds, C 60 seconds, and D 90 seconds.

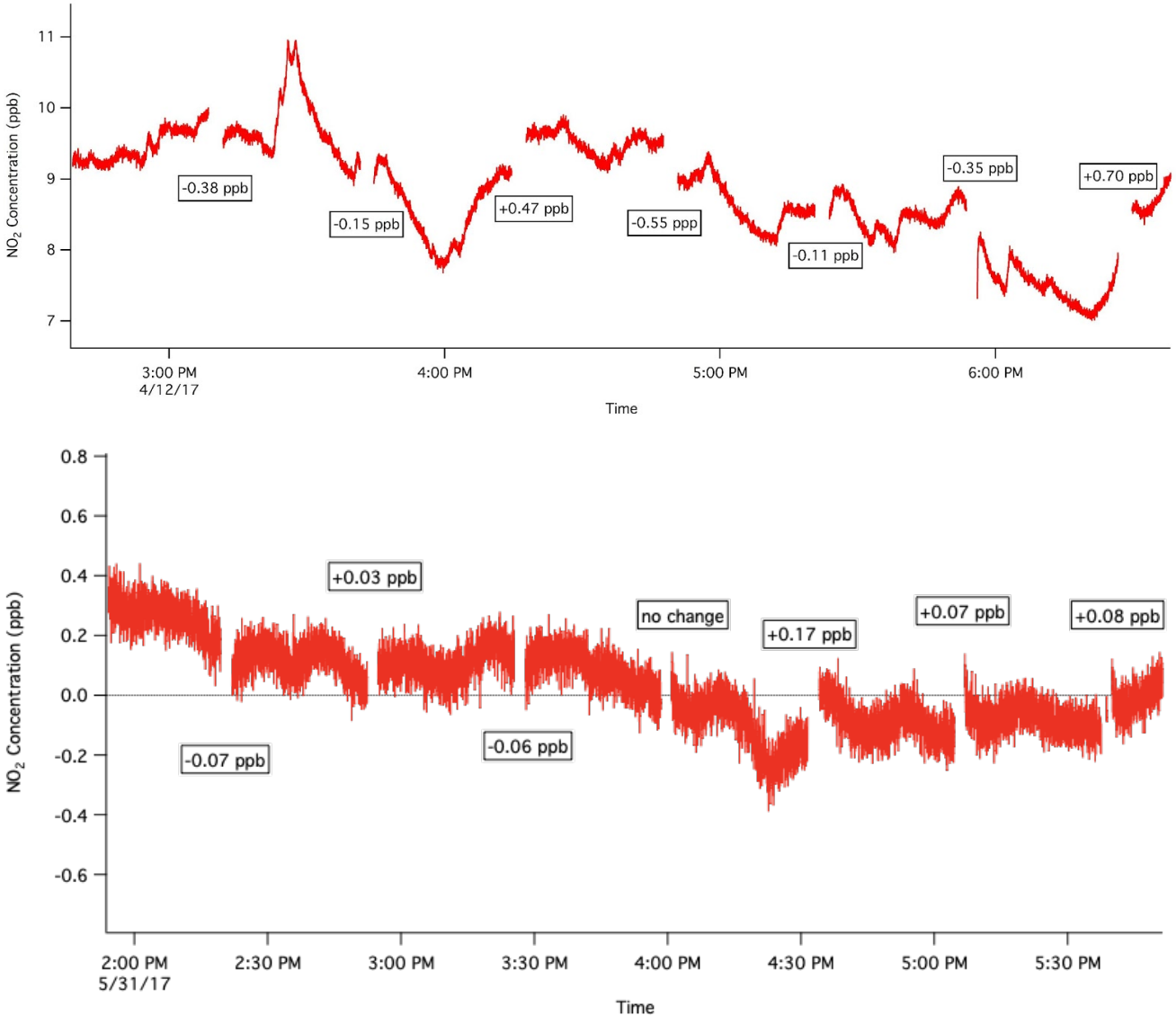

Figure S3. CRDS running for 4 hours on room air (upper panel) or zero air (lower panel). Seven instrument zeroes are visible across each timeseries to show the typical changes in signal. For the detection limit analysis included in the manuscript, the standard deviation of the zero signal measured over the full length of the lower panel was calculated, and found to be σ_{zero} = 0.16 ppb.

Table S1. Rate constants for different species used in kinetics model.

Dissociation / Recombination Reactions	**Dissociation rate parameters (Day et al., 2002, Table 1)**	**Recombination parameters ("JPL Data Evaluation" 2015, Table 2-1)**

	k_o[a]	a[a]	k_h[b]	b[b]	k_o^{300}[c]	n[c]	k_∞^{300}[d]	m[d]
PN↔ NO_2 + $CH_3C(O)OO$	$4.9x10^{-3}$	12100	$4x10^{16}$	13600	$9.7x10^{-29}$	5.6	$9.3x10^{-12}$	1.5
AN↔ NO_2 + C_2H_5CO or C_3H_70	-	-	$3.16x10^{16}$	20129	$2x10^{-27}$	4	$2.8x10^{-11}$	1
HNO_3↔ NO_2 + OH	$(1.82x10^{-4})$ $(T/298)^{-1.98}$	24004	$2x10^{15}$	24658	$1.8x10^{-30}$	3	$2.8x10^{-11}$	0
Loss Reaction	**Rate constant**							
OH → walls[e]	46 s^{-1}							
n-C_4H_9O + O_2 → products[f]	$(8.9x10^{-14})(e^{-550/T})$ cm^3 $molecule^{-1}$ s^{-1}							

a. Low pressure limit $k_o(T) = k_o exp(-a/T)$, where T is temperature in Kelvin, cm^3 $molecule^{-1}$ s^{-1}

b. High pressure limit $k_h(T) = k_h exp(-b/T)$, where T is temperature in Kelvin, cm^3 $molecule^{-1}$ s^{-1}

c. Low pressure limit $k_o(T) = k_o^{300} (T/300)^{-n}$, where T is temperature in Kelvin, cm^3 $molecule^{-1}$ s^{-1}

d. High pressure limit $k_\infty(T) = k_\infty^{300}(T/300)^{-m}$, where T is temperature in Kelvin, cm^3 $molecule^{-1}$ s^{-1}

e. Knopf, Pöschl, and Shiraiwa 2015

f. IUPAC evaluation, reaction RO_5, http://iupac.pole-ether.fr/

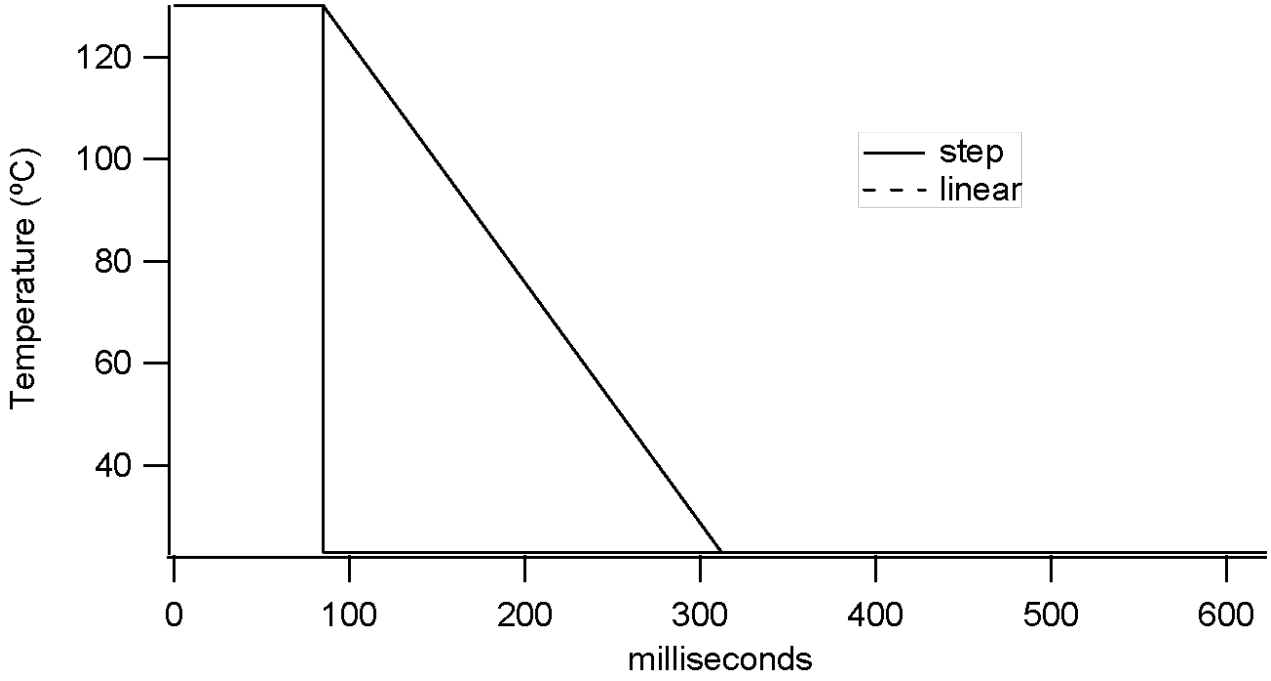

Figure S4. Two considered models of cooling rates in the quartz tubing after the PN oven.

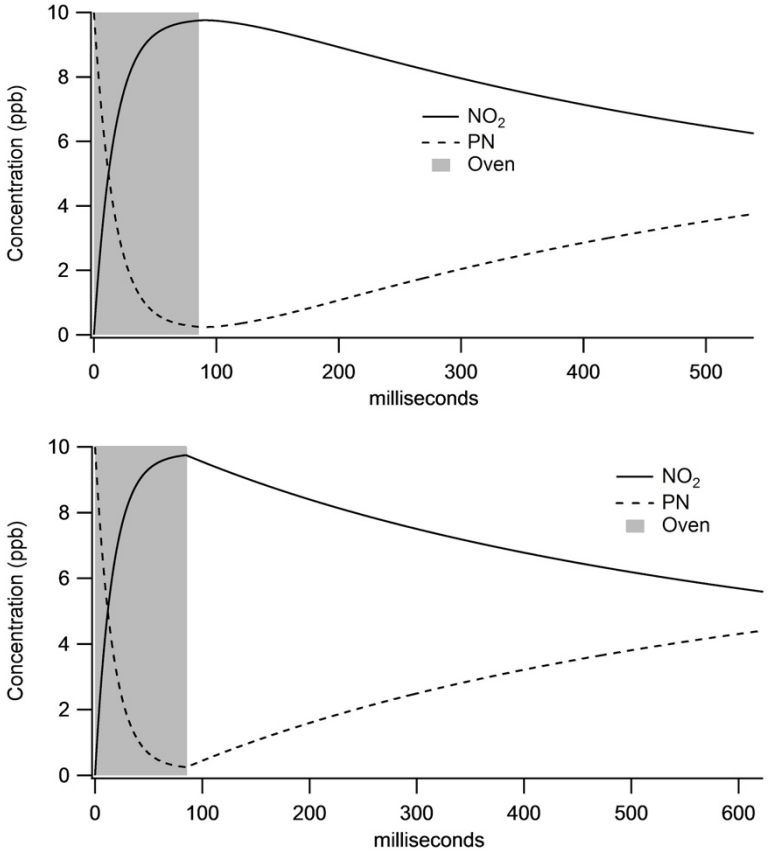

Figure S5. Model of PN dissociation through an oven at 120ºC, using both step function (left) and linear temperature decay (right). Shaded region is the heated portion of the oven.

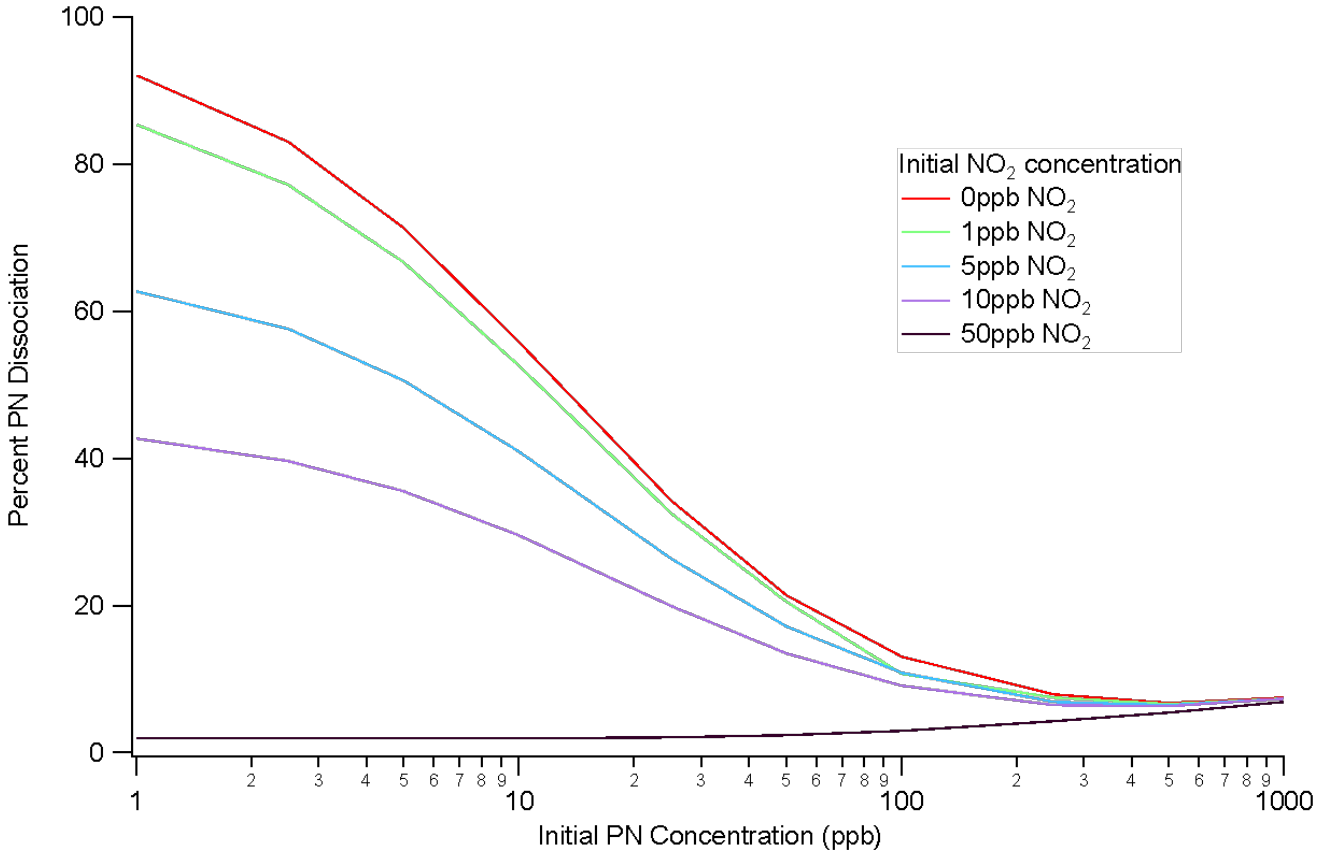

Figure S6. Percent PNs detected at CRDS at different initial concentrations of PNs and NO_2. Most work is done in the lower concentration range of both PNs and NO_2, where the percent of PNs that remain dissociated to the detector is relatively higher; however we note the recombination effect here is larger than for ANs or HNO_3 (see Figure S7). Percent dissociated is equivalent to percent detected.

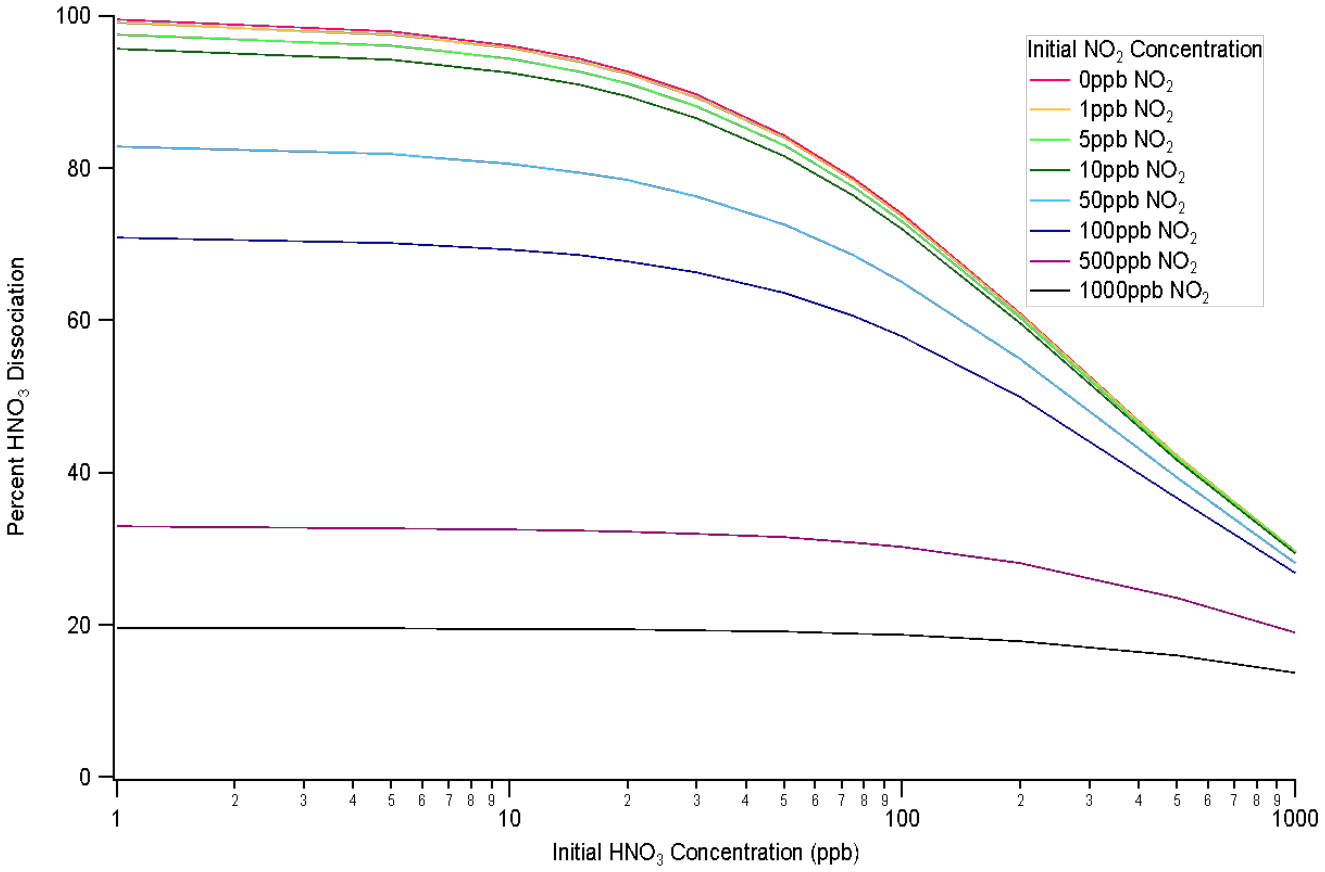

Figure S7. Percent HNO_3 detected at CRDS at different initial concentrations of nitric acid and NO_2. Most work is done in the lower concentration range of both HNO_3 and NO_2, where the percent HNO_3 that remains dissociated to the detector is high. Percent dissociated is equivalent to percent detected.

625

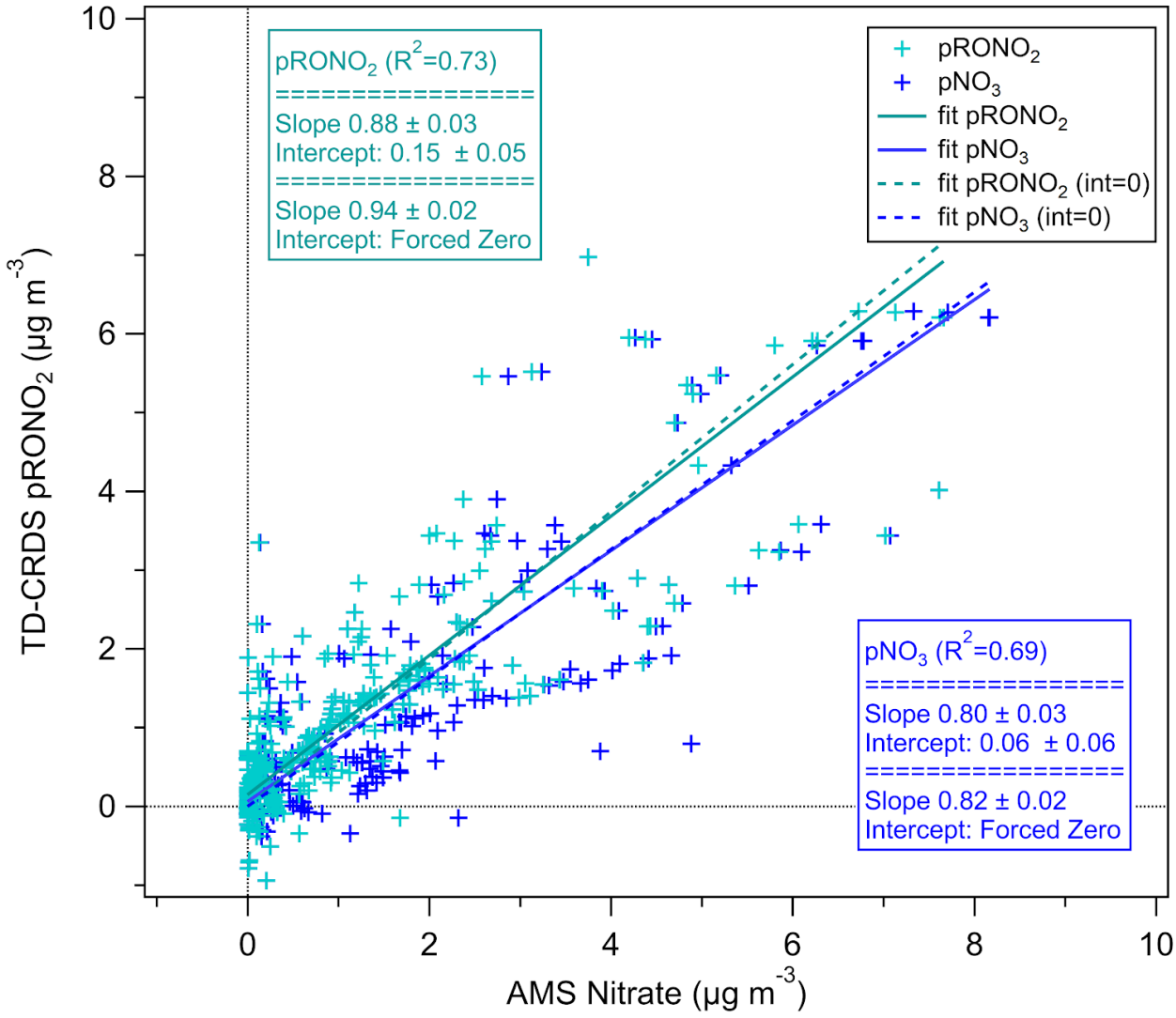

Figure S8. TD-CRDS organic nitrate vs AMS total nitrate (pNO_3) and apportioned organic nitrate fraction ($pRONO_2$).